The Identification of Roof Bar Noise Sources using Acoustic Beamforming in a Full-scale Automotive Wind Tunnel

Oliver Smith, Nicholas Oettle

Aeroacoustics - Vehicle Efficiency
Jaguar Land Rover Ltd.
Gaydon
Warwickshire
CV35 0RR
United Kingdom

osmith@jaguarlandrover.com
noettle@jaguarlandrover.com

Abstract: Increasingly, across global markets, external accessories such as roof cross bars are being fitted by vehicle owners not only for temporary functional use but also semi-permanently for their aesthetics. The aerodynamic interaction of the flow around accessories, such as roof bars, and their parent vehicle can generate significant aeroacoustic noise sources. These may be aeolian or highly tonal in nature and of particular annoyance to the occupants. This, in combination with the industry trends of increased refinement, means the aeroacoustic performance of accessories is becoming more important to vehicle designers as the end user expectation and usage case changes.

This paper presents the capture and visualisation of typical aeroacoustics phenomena and acoustic error states that can present around roof bars fitted to a production vehicle. These are namely tonal sources due to vortex shedding and Helmholtz resonance, as well as the broadband sources from the interaction of the roof bars, their mounting system, and the parent vehicle.

The visualisation is conducted by applying both acoustic beamforming in a full-scale aeroacoustic wind tunnel and additionally the use of a validated Lattice Boltzmann Method CFD code. This enables key phenomena to be identified thus demonstrating that the toolsets can be used to design-out or optimise the form to minimise dissatisfactory performance.

1 Introduction

As passenger vehicles become more refined, occupants are becoming more sensitive to any increase in cabin noise above that experienced in their standard vehicle. This applies to both broadband and discrete tonal sounds and is exacerbated by the transition to electrified powertrains [1].

One potential source of additional noise is the fitment of roof bars to a vehicle. Traditionally, accessories such as roof bars have been fitted by the user temporarily and for functional purposes such as transportation of large items or leisure activities. This voluntary fitment has typically come with some acceptance of a temporary increase in wind noise. Additionally, in some global markets, users are now fitting accessories semi-permanently for aesthetic appeal and vehicle personalisation. In these latter cases, tolerance to accessory noise may be lower and may lead to customer dissatisfaction and complaint if it is not considered and minimised during the engineering of the vehicle and accessory designs.

A common approach to designing roof bars is to utilise an existing bar profile from a catalogue of extrusions. Much of the established literature highlights that, whilst these profiles may have been empirically developed to mitigate the risk of certain aeroacoustic phenomena [2][3][4][5], they are typically not optimised for refinement explicitly, either in isolation or in context of the airflow around the parent vehicle. This is also true of the mounting system. As a result, roof bars can deliver sub-optimal aeroacoustic performance, delivering elevated broadband noise or excessive aeolian tonal sounds and may be objectionable to the user.

The aim of this paper is to demonstrate the use of large microphone array beamforming to identify, localise and visualise some typical aeroacoustic phenomena that may occur over a roof bar system mounted to the parent vehicle. These include a combination of the broadband noise sources and deliberately induced tonal error states, in order to demonstrate breadth of the toolsets' capabilities. The described methods can allow engineers to identify and mitigate or minimise the noise-generating features during the design process.

2 Methodology

2.1 Acoustic Beamforming using the FKFS beamforming array

Acoustic beamforming is a visualisation and measurement technique used to extract and identify noise sources within a broadband far-field soundscape, in both frequency and space.

The signal-processing method implemented in this investigation is *delay and sum* beamforming, working with target locations on an investigation area in this case nodes on a planar mesh at a constant distance from the array [6] [7]. There are two stages to the process: time shifting the noise signals from each microphone, based on the knowledge of the speed of sound and the microphone position relative to the target location; followed by the summation of the total number of microphone signals. For a target location when a noise source is present, the sum of the signals will combine constructively, resulting in a high total signal. For target locations where a noise source is not present, the combination of signals will be at a low level.

The acoustic beamforming system of the FKFS wind tunnel comprises two arrays: a 168 microphone array positioned directly above the vehicle, and a 144 microphone side array, which can be positioned on either side of the vehicle [8] [9] [10]. Both arrays are outside of the jet of the wind tunnel to avoid wind interference and consequently a correction is applied to take into account the refraction effects of the shear layer at a given wind speed. A general image of the arrays within the wind tunnel is shown in Figure 2.

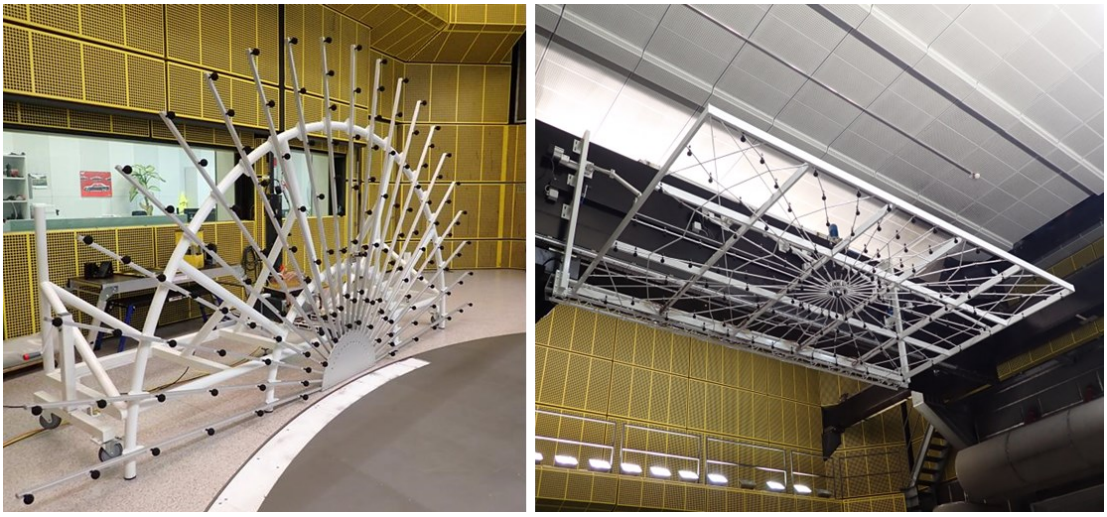

Figure 2: The top and side acoustic arrays of the FKFS wind tunnel

The microphones of each array were connected to separate, time-synchronised, Siemens SCADAS front ends. In addition, a further synchronised front end was positioned in the vehicle, connected to two half-inch microphones positioned between the front and rear seat positions. These were used as reference signals for coherence-based signal processing, allowing exterior noise data to be presented that more coherent to the noise heard inside the cabin and hence identifying exterior sources more relevant to the vehicle occupant. [9] [10]. Acoustic data were recorded for 60 seconds and processed using Siemens Simcenter Test.Lab software.

In addition to the two correlation microphones to support the array measurements, interior cabin noise data were also recorded using HEAD Acoustics HMS IV binaural heads, in each of the four seat positions.

2.2 CFD Simulations

To support the engineering of vehicle accessories prior to physical models or parts being available, the phenomena described in this paper can also be captured virtually, using the commercially available CFD code PowerFLOW.

For all simulation examples, the methodology broadly follows the toolset's best practice for capturing and assessing vehicle greenhouse wind noise with some modifications to resolution and measurement for the specific application [11].

2.3 Vehicle and Test Conditions

The vehicle was tested experimentally using the FKFS full-scale aeroacoustic wind tunnel of the University of Stuttgart in Germany [12][13]. The comparable virtual vehicle model was externally complete, suitably detailed and meshed to the tool's best practice for aeroacoustic simulation. An image of the physical and virtual vehicle are shown in Figure 3.

Figure 3: The vehicle under test in the wind tunnel and virtual representation

The virtual and physical tests were conducted at a variety of onset flow speeds between 80 and 160 kph, covering a range of typical driving conditions.

The content of this paper focusses the roof bar system in three configurations: the series production installation in order to characterise and visualise roof bar noise with the tools demonstrated; with the rubber T-track cover removed and replaced with a smooth surface, in order to induce von Kármán vortex street in the wake and mid-frequency howling; and with the rubber cover removed to expose the T-track cavity to the airflow, in order to induce Helmholtz resonance and whistling.

3 Results

3.1 Baseline Roof Bars

As a baseline, the production roof bars were first evaluated. Whilst they are audible in the cabin, they are viewed to perform acceptably and without error state, so this first use case demonstrates how the toolsets can be used to identify specific noise sources within the broadband – potentially providing scope for further optimisation. Figure 4 shows a rendering of the installed bars. Note the castellated rubber 't-track' cover strip along the top surface.

Figure 4: A rendering of the baseline roof bars

Figure 5 shows the resulting interior noise spectra measured at the front microphone position versus wind speed in the wind tunnel. The wind speed in the wind tunnel was progressively increased at a rate of 1 kph/s, during which the interior acoustic data was continuously recorded.

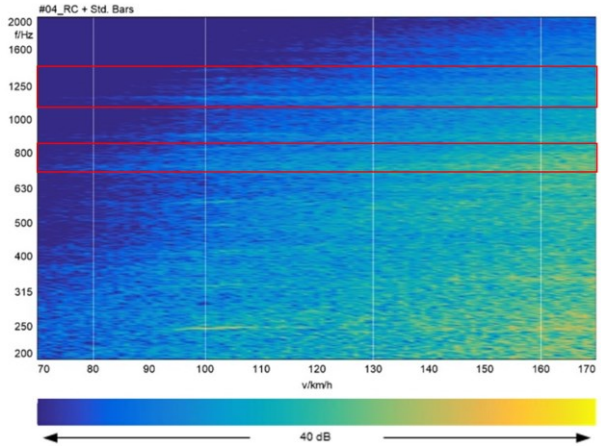

Figure 5: 3D noise map of interior noise spectra versus wind speed for baseline roof bars. 800Hz and 1.25 kHz one third octave bands bound by red boxes.

The figure shows an overall progressive increase in SPL with flow speed, as shown by the colours of the map becoming progressively lighter as the wind speed increases. As these roof bars are considered to perform acceptably for this vehicle, the features and acoustics sources of note are subtle but are highlighted by the horizontal striping patterns on the graph. The frequency of these generally do not change with flow speed, indicating that the sources increase in a broadband manner.

The examples that follow investigate the subtle stripes within both the 800 Hz and 1.25 kHz one-third-octave bands (as highlighted in Figure 5) in order to demonstrating the toolsets' abilities to identify specific noise sources within the broadband soundscape.

Considering the contribution beamforming contours, presenting data coherent to the interior reference microphone in the front of the cabin, for the 800 Hz one-third-octave at 160 kph (Figure 6), it is clearly highlighted that the cross bars as the dominant acoustic source of the striping seen in Figure 5. It is also notable that the rear bar presents a stronger source than the front one. This is due to the wake of the front bar interacting with the rear.

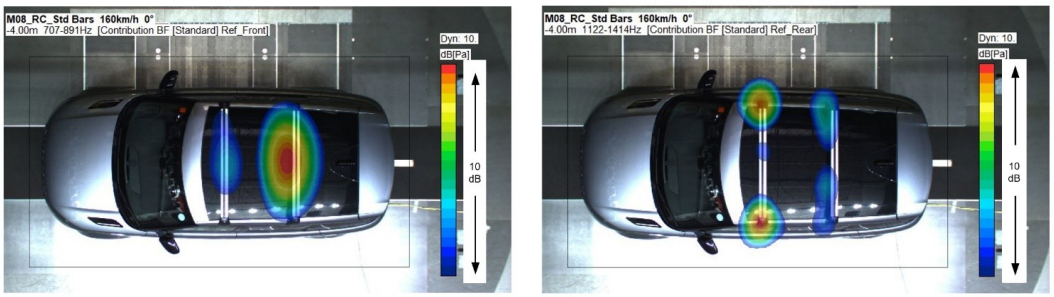

Figure 6: Contribution beamforming of baseline roof bars (800 Hz third-octave left, 1.25 kHz right)

If the performance at 800Hz were deemed to be unacceptable, this result would direct the engineers to consider either the bar profile or relative position of the rear bar to the front in order to reduce the noise generated. When the same correlated beamforming contour results are considered for the 1.25 kHz one-third-octave band, it is instead apparent that the mounting feet are the dominant noise source. This result would guide engineers to further optimise the fairings of the mountings if there was a desire to reduce the noise in these frequencies.

Comparable results are also obtainable from the CFD method, highlighting the dominant noise sources at both frequency bands in Figure 7.

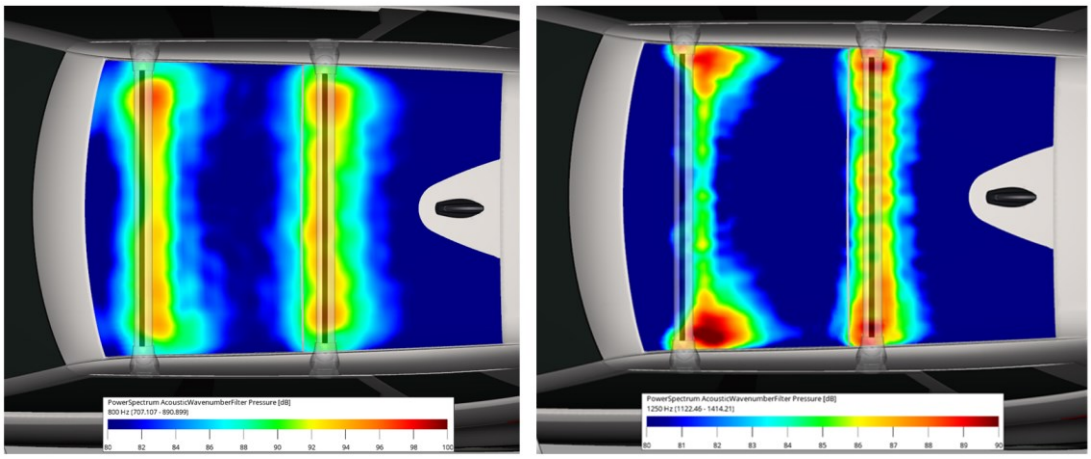

Figure 7: One-third octave band filtered acoustic dB maps of the production roof bars (800 Hz left, 1.25 kHz right)

The use of these techniques demonstrates that even with the cross bars performing in an acceptable manner, the most significant audible noise sources can be identified and could allow further optimisation of bar shape and position, and perhaps more significantly optimisation of the fairing around the mounting feet.

3.2 Smooth Roof Bars

On an aerofoil, at higher Reynolds' numbers (greater than 10^5 based on chord length) or where the boundary layer on an aerofoil is tripped, the boundary layer becomes turbulent. For an aerofoil with a finite thickness where the base pressure is low, the boundary layers from the upper and lower surfaces can interact, forming the well-known von Kármán vortex street behind the aerofoil. The fluctuating unsteady pressures in the wake generate a noise source consistent with that of a dipole [14].

In the case of roof bar profiles that are designed primarily for load carrying, the profile is often rather blunt. This can lead to the aforementioned vortex shedding, unless alleviated through approaches such as the addition of a castellated strip on the baseline bars.

To investigate how the acoustic sources may be visualised in the case of a bar that presents the blunt trailing edge tonal noise, the castellated strip of the baseline bars was removed with the open T-track covered forming a continuous aerofoil profile. This was achieved using thin aluminium tape in the wind tunnel, whereas in the simulation this was achieved though modification to the geometry, as shown in Figure 10.

Figure 10: A rendering of the roof bars with the T-track cover removed and the cavity tangentially covered

Figure 11 shows the interior noise map during a speed sweep in the wind tunnel. A clear tonal feature is visible on the noise map, increasing monotonically with speed, with the peak level remaining relatively constant.

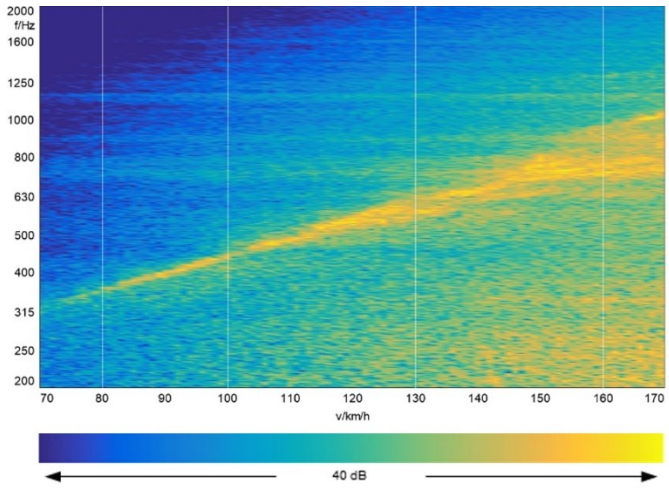

Figure 11: 3D noise map of interior noise spectra versus wind speed for roof bars with T-track cover removed and smoothed over.

Von Kármán vortex shedding can be characterised using non-dimensionalised frequency as the Strouhal number, St, defined by Equation 1, where f is frequency, U is oncoming flow speed and h is a characteristic dimension of the profile.

$$\mathrm{St} = \frac{fU}{h}$$

Equation 1: Strouhal number definition

By non-dimensionalising frequency in terms of Strouhal number, at four sampled velocities, the peak tonal shedding frequency at each flow speed collapse onto a single Strouhal number (Figure 12). This indicates the tone is due to periodic coherent vortex shedding and scales with vehicle velocity. Given the order of magnitude assumptions in terms of characteristic oncoming flow speed and dimension of the bars, the resulting Strouhal number between 0.1 and 1 is consistent with the literature [15] [16].

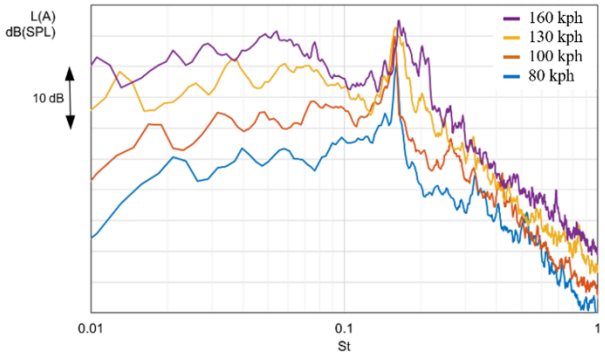

Figure 12: Interior noise spectra at discrete wind speeds of the roof bars with T-track cover removed and smoothed over, based on Strouhal number

Figure 13 shows contribution beamforming contours of the smooth roof bars at 160 kph, presenting data from the 800 Hz third-octave band, which captures the main shedding peak frequency at this speed. capturing shedding peak at 160 kph.

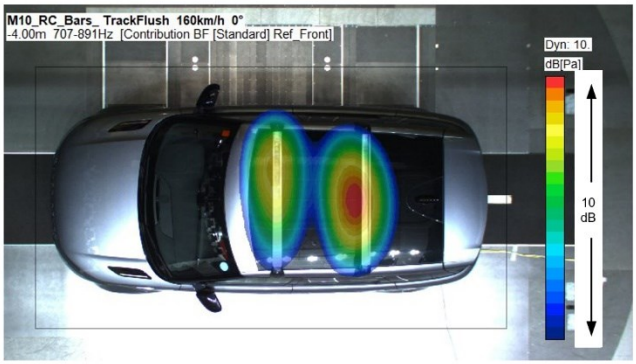

Figure 13: Contribution beamforming of roof bars with T-track cover removed and smoothed over (800 Hz third-octave)

The noise sources from the bars display significantly increased noise generation when compared to Figure 6, particularly from the front bar. This clearly identifies the noise issue, directing development to changing the bar profile (by adding castellated strips or otherwise) in order to reduce this noise.

The regular vortex shedding, characteristic of the von Kármán vortex street, is shown in the velocity magnitude slice from the CFD simulation at 160 kph of Figure 14.

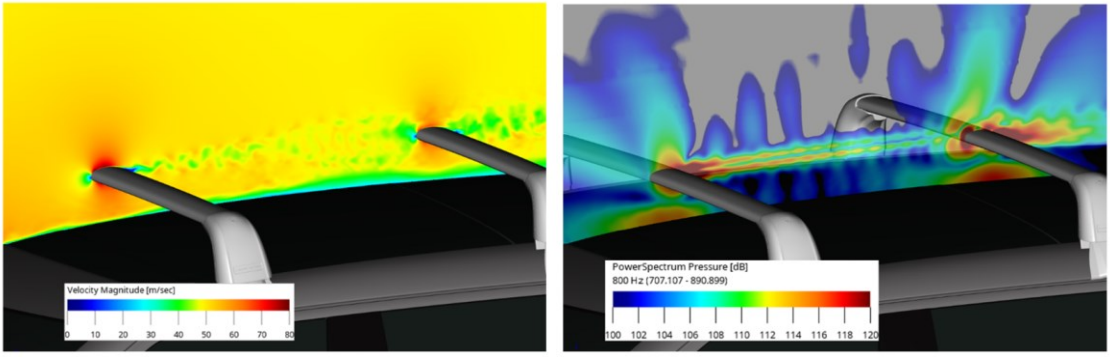

Figure 14: y=0 slice at velocity magnitude (left) and 800 Hz third-octave pressure fluctuations (right) at 160 kph of smooth roof bars

The level of shedding is greater from the rear bar, likely due to a degree of constructive interference with the shedding from the front bar, since the bars are of the same profile and consequently shed at the same Strouhal number. The increased noise generation from the rear bar is identified in the 800 Hz third-octave pressure fluctuation slice, showing good agreement with the equivalent beamforming image of Figure 13, with virtual and physical methods able capture the key aeroacoustic phenomena to guide engineers in performance enhancement.

3.3 Open Channel Roof Bars

Another common issue that can occur in roof bar design are high-frequency tonal whistles due to open slots and cavities. Roof bars commonly have such slots to position mounting hardware for load carrying, and manufacturers often provide strips to cover these to prevent acoustic issues. To investigate how these may be visualised, the castellated strip of the baseline bars was removed exposing the open T-track as presented in Figure 16.

Figure 16: A rendering of the roof bars with the T-track open

As before, the bars were added to the vehicle in the wind tunnel and continuous interior noise measurements were made as the wind speed was progressively increased. The resulting noise map, comparable to those measure for the previous two roof bar configuration is shown in Figure 17.

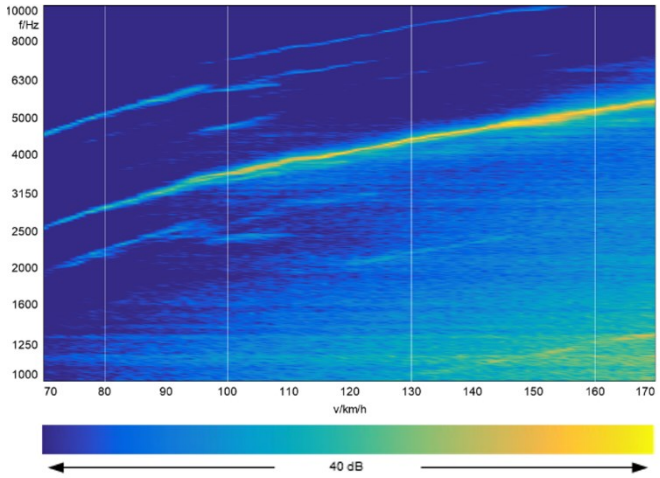

Figure 17: 3D noise map of interior noise spectra versus wind speed for roof bars with T-track open. Strong tonal features are visible and scale with vehicle velocity.

A number of tonal features and harmonics are visible, scaling with wind speed. Cavity noise is produced from a coupling of aerodynamic excitement with an acoustic response. In this case, the mechanism is similar to that of sunroof boom [17]. Here, the transient characteristics of a shear layer instability over a cavity excite an acoustic mode of the open roof bar cavity [18]. Multiple tonal peaks can be generated, due to higher order Rossiter modes coupling with the Helmholtz modes at different speeds. In addition, the roof bars themselves being of finite length have multiple acoustic modes which may also be excited.

Figure 19 shows contribution beamforming contours of the roof bars with the T-track opened at 100 kph, presenting data from the 4 kHz third-octave band, capturing the main shedding peak frequency at this speed.

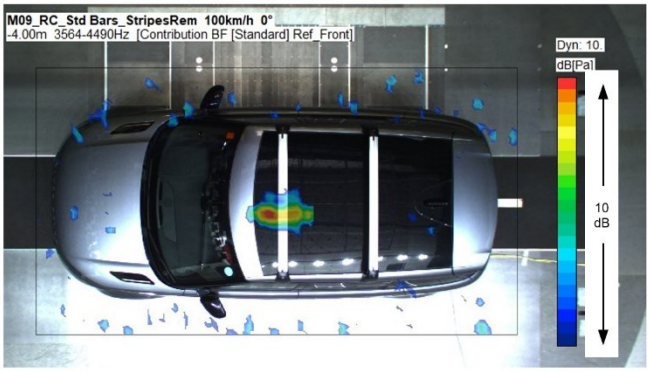

Figure 19: Contribution beamforming of roof bars with T-track open (4 kHz third-octave).

The wind tunnel beamforming contours shows a high-level noise source from front bar, near the centreline of the car. The nature of this is possibly due to the tonal nature of the source coupling with a longitudinal mode of the open roofbar section, with the antinode present at this point.

Visualising the Helmholtz resonance whistling virtually is also possible though the use of slices though the fluid domain. Figure 21 depicts a single frame in the transient simulation shaded by the local time derivative of pressure. The strong acoustic pressure fluctuations from the whistle monopole are clearly visible radiating from the front bar, matching the spatial location observed through acoustic beamforming in the wind tunnel.

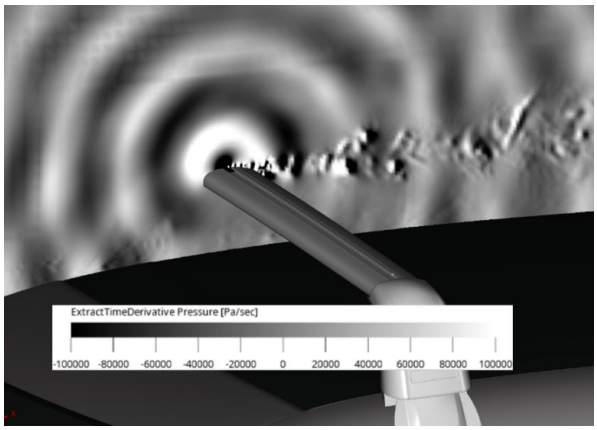

Figure 21: Snapshot of y=0 slice with the time derivative of pressure shown.

4 Conclusions

The aim of this paper was to demonstrate the application of large microphone array beam forming to visualise the aeroacoustic performance of roof bars when fitted to a parent vehicle. This includes the identification of deliberately induced aeroacoustic error states that may occur on such systems during development and that would be objectionable to the consumer.

Taking the measured data from inside a vehicle cabin, a number of acoustic features were identified in the acoustic spectra. Through the use of the acoustic array, the source of these features were clearly identified, providing direction to the development process, focussing development to maximise customer benefit. In addition, acoustic beamforming was demonstrated to identify two common roof bar aeroacoustic error states that may occur in development or when exploring a new concept.

Through the use of a prototype parts and an aerodynamic buck or virtually in CFD simulations, these methods therefore may allow for earlier assessment of new cross bar profiles, novel design concepts or vehicle pairings, ultimately reducing the risk of late change and costly empirical fixes being developed.

5 Reference list

1. Oettle, Nicholas, and David Sims-Williams. "Automotive aeroacoustics: An overview." Proceedings of the Institution of Mechanical Engineers, Part D: Journal of Automobile Engineering 231, no. 9 (2017): 1177-1189.
2. Karbon, Kenneth J., and Urs D. Dietschi. "Computational analysis and design to minimize vehicle roof rack wind noise." SAE transactions (2005): 649-656.
3. Lee, Myunghan, Jeonghan Lee, and Daehoon Kim. Reduction of Aeolian Noise from Roof Rack Crossbars Using Asymmetric Cross-Section Geometry. No. 2002-01-1275. SAE Technical Paper, 2002.
4. Massarotti, Mauricio R., and William R. Wolf. Understanding the aeroacoustic noise mechanisms and noise control techniques of roof rack systems. No. 2018-36-0025. SAE Technical Paper, 2018.
5. Senthooran, Sivapalan, Bradley D. Duncan, David Freed, Dena Hendriana, Robert E. Powell, and John Nalevanko. "Design of roof-rack crossbars for production automobiles to reduce howl noise using a lattice Boltzmann scheme." SAE Transactions (2007): 1974-1982.
6. J. Christensen and J. Hald, “Technical review: Beamforming,” Brüel Kjær, Tech. Rep., 2004.
7. H. Vickers, “The enhancement of beamforming analysis on road vehicles by the introduction of cross-correlation functionality,” Master’s thesis, Durham University, 2017.
8. Blumrich, R, M. Riegel, N. Oettle, H. Vickers, B. Verrecas, A. Finez, O. Minck, “A Comparison of Wind Tunnel Array-Based Aeroacoustic Measurement Techniques”. International conference on vehicle aerodynamics 2018, Birmingham, 16 – 17 October, 2018.
9. Riegel, M., Reinhard Blumrich, Olivier Minck, Bart Verrecas, Nicholas Oettle, Harriet Vickers. “New Large Microphone Array at the FKFS Wind Tunnel”. 12th FKFS conference, Stuttgart, 1 – 2 October, 2019.
10. Siemens Digital Industries Software, Press release: FKFS achieves a winning difference for its aeroacoustic wind tunnel from Siemens Simcenter. (2019)
11. Smith, O. and Oettle, N., “Visualisation of Roof Bar Noise Sources through the Use of Acoustic Beamforming and Computational Aeroacoustics,” SAE Technical Paper 2023-01-0840, 2023, doi:10.4271/2023-01-0840
12. Blumrich, Reinhard, Nils Widdecke, Jochen Wiedemann, Armin Michelbach, Felix Wittmeier, and Oliver Beland. "New FKFS technology at the full-scale aeroacoustic wind tunnel of University of Stuttgart." SAE International Journal of Passenger Cars-Mechanical Systems 8, no. 2015-01-1557 (2015): 294-305
13. Künstner, Rudi, Jürgen Potthoff, and Ulf Essers. "The aero-acoustic wind tunnel of Stuttgart University." SAE transactions (1995): 1119-1135.
14. Hansen, Colin H., Con J. Doolan, and Kristy L. Hansen. Wind farm noise: measurement, assessment, and control. John Wiley & Sons, 2017.
15. Blake, William K. Mechanics of flow-induced sound and vibration, Volume 2: Complex flow-structure interactions. Academic press, 2017.

16. Brooks, Thomas F., and T. H. Hodgson. "Trailing edge noise prediction from measured surface pressures." Journal of sound and vibration 78, no. 1 (1981): 69-117
17. Oettle, Nicholas, Mohammed Meskine, Sivapalan Senthooran, Andrew Bissell, Gana Balasubramanian, and Robert Powell. "A computational approach to assess buffeting and broadband noise generated by a vehicle sunroof." SAE International Journal of Passenger Cars-Mechanical Systems 8, no. 2015-01-1532 (2015): 196-204
18. Rossiter, J.E., 1964, Wind-tunnel experiments on the flow over rectangular cavities at subsonic and transonic speeds, Aeronautical Research Council Reports and Memoranda, Technical Report 3438, (1964)